Alaska Hydro-Flow Generator

Project team 19
Jacob Gore, Eric Lankheet, Jason Riggs, Ching-shih Yang

ME 450: Design and Manufacturing III
Winter 07' Final Report
Professor Katsuo Kurabayashi
4-17-2007

Table of Contents

Abstract

The University of Michigan's Hydrodynamic Laboratories has requested our assistance in designing and developing a portable hydroelectric generator for supplying power to remotely located Alaskan research camps using nearby rivers. The design specifications required our product to be portable and robust enough for the given environment. To meet these specifications, we generated and analyzed various concepts to ultimately select a concept that uses two turbine blades in series that will drive an electric generator. Using a generator and blade test rig, we estimate that the finished product will be able to produce approximately 1 kilowatt of power.

Introduction and Problem Statement

At the Bering Glacier in Southwest Alaska, valuable research is being conducted every summer on the natural evolution and future preservation of the area. However, because of its remote location, research camps and native villages in the region do not have a ready source of power. Thus, researchers have been relying on gasoline powered generators to fulfill their power needs. To supply these generators, bush planes are used to transport gasoline. This method of transportation presents a possible danger both to those transporting the gasoline and to the environment. An accident that resulted in the death of a bush plane pilot has proved this danger to be real. To deal with this problem, the research camp must be able to find or develop an alternate source of energy that does not require transportation that could be potentially dangerous.

To tap in to the energy available in the surrounding environment, researchers at the University of Michigan's Marine Hydraulic Laboratory (MHL) observed that the nearby river systems possess far more than enough energy that could be harvested to power the camps. As shown in Figure1 below, the melting of glaciers in the region result in channels of water that supply the river system in the surrounding region.

Figure 1: A Channel of Water Formed by Melting Ice (courtesy of MHL)

Since the most amount of ice melts in the summer, the river flow is also the fastest at that time. Therefore, research activities, which are carried out in the summer, could take advantage of this increased flow to produce the necessary power requirements. Supplied by the melting ice, these rivers have an estimated flow rate of 1,400 to 2,500 m^3/s, which corresponds to a water speed of 2 to 4 m/s.

MHL researchers have proposed that a hydroelectric generator could be developed to environmentally harvest the power from the river flow. To satisfy the camps' power needs, the hydroelectric generator system would need to provide 10 ~ 30kw of power. Also, to be easily transported, the hydroelectric generator would need to weigh less than 500 lbs. Due to floating ice blocks and sediment in the river, the portion of the hydroelectric generator system in the water needs to be very robust and durable. MHL has presented these requirements to us for guiding our design and manufacturing process.

Information Search

To begin the design process, we researched information and patents for portable hydroelectric generators to better understand the system that we need to design. We found that most portable hydroelectric generators on the market are designed to generate electricity from a vertical downward fluid flow in a pipe or tube. These portable hydroelectric generators are meant to produce lower power than that which is needed for an entire research camp. Also, these products are typically designed for high head, low flow rate environments. Figure 2 below shows a picture of such a product.

Figure 2: Platypus Power's M1 Micro Hydroelectric Generator (Max: 800 Watts) [1]

Customer Requirements and Engineering Specifications

Since the portable hydroelectric generator will be operating in a remote location with a harsh environment, MHL has specified several requirements that the product will need to meet. The product will need to be able to withstand the harsh environment and be portable enough to be transported by a bush plane. Also, the generator will need to be able to produce enough power to decrease the amount of gasoline consumed by the camp. The specific requirements and corresponding engineering specifications are as follows:

1. Portable: Less than 500 lbs.; able to be carried by a bush plane

2. Durable: Needs bearings that won't be ruined by the sediment and debris deflection device for deflecting ice blocks; needs to last for a long time.
3. Consistent power output: Need system to control power output to a constant value.
4. Ability to store excess output: Could use a hydraulic accumulator, batteries, or other such components for energy storage.
5. Small environmental impact: Made of components that won't have a negative impact on the environment during or after usage.
6. Easy setup: All components to system must be easily assembled on-site.
7. Multi-use: System would preferably include methods of utilizing excess energy that will improve the users' standard of living.
8. Safe: All electrical and hydraulic systems must be safe to the users.
9. Robust: System should be able to compensate for the wide range of river flow rate.
10. Low cost: Whole system should cost less than $4,000.

The specific requirements and engineering specifications are included in the quality function deployment shown below as Figure 3.

Quality Function Development (QFD)

Relationships

++ Strong Positive
+ Medium Positive
- Medium Negative
-- Strong Negative

(+) => more is better
(-) => less is better

Key:
9 => Strong Relationship
3 => Medium Relationship
1 => Small Relationship
(blank) => Not Related

	Weight*	Power output(+)	Turbine Size(+)	Hydraulic Fluid(-)	Energy Storage(+)	Foreign objects deflected(+)	Reservoir size(+)	Weight(-)	Wide water flow range(+)	Component life span(+)	Cost(-)		Benchmarks: *Proposed Design*	*Platypus*	*Aquair Underwater Turbine*
Portable	9		3				3	9					3	4	5
Durable	7					9				9			5	4	2
Consistent power output	8	9	3			3			1				5	3	2
Ability to store excess output	8	3			9								5	1	1
Small environmental impact	8			9									4	3	3
Easy setup	5		1			1	3	3					3	2	3
Multi use	4			3									4	1	1
Safe	10					1		1		3			4	4	4
Robust	9	1							9				4	2	1
Low Cost													4	2	4
Measurement Unit		KW	m	NA	MJ	%	L	lbs	m/s	yrs					
Target Value		10	0.5	NA	162	100	56	500	2	5					
Importance Rating		2	8	6	7	3	9	1	5	4					
Total		105	56	84	72	102	42	106	89	93	0				
Normalized		0.14	0.07	0.11	0.10	0.14	0.06	0.14	0.12	0.12	0.00				
Proposed Design		4	4	5	4	4	3	2	4	3	3				
Platypus		5	3	NA	2	1	NA	2	3	4	1				
Aquair Underwater Turbine		1	2	NA	1	1	NA	5	5	2	3				

Scale of 1-5
5 is best

*Weights are figured on a scale of 1 to 10
(ten being most important)

Figure 3: Quality Function Deployment

Preliminary Concept

Before requesting our assistance, researchers from MHL have already developed a concept for the energy extraction component of the system. Figure 4 below presents this concept. The twin blades in this concept would allow for more power extraction from the river flow. The spinning of the blades would actuate the hydraulic pump, which would then send pressurized fluid up to the rest of the hydroelectric system. With this concept, most of the electrical components could be kept safe and dry on land. Another option is that the twin blades could directly run a generator instead of a pump. In that case, an electrical line would directly carry current from the generator up to the camp to be used.

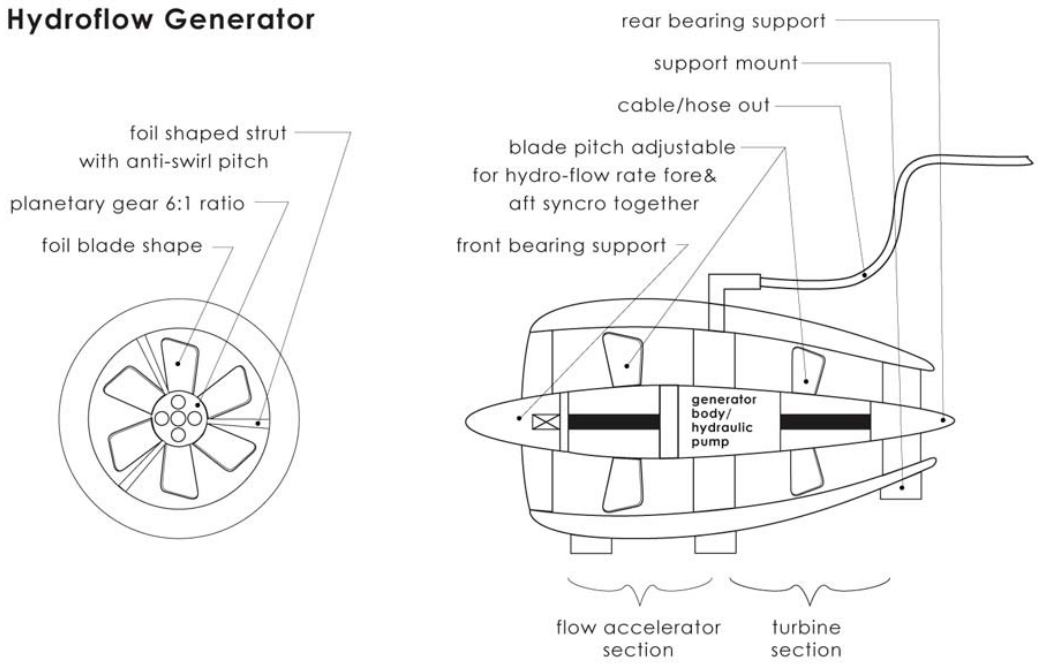

Figure 4: MHL's Hydroflow Generator Concept (courtesy of MHL) [1]

Along with the current concept for the hydroflow generator, our team has determined that the entire hydroelectric generator system could be setup in two ways. In the first method, the system would directly convert the rotational power from the spinning blades to electrical power by using an electrical generator. This method would result in an approximately constant flow of electricity from the generator, which would most likely need to be stored in batteries in order to be useful to the camp. Also, this first method would very likely require electrical components like the generator to be underwater. The second method for setting up the system would essentially involve storing the power from the hydroflow generator as pressure in a hydraulic accumulator. Then, when desired, the accumulated pressure could be used to complete a hydraulic circuit with a commercial hydraulic generator, which would then generate the necessary power.

Concept Generation

To generate possible concepts for our generator system, we first determined that the system will need to be made of 3 or 4 components: energy extraction component, energy transfer component, an optional energy storage component, and an energy dissipation component. We continued by producing several concepts for each component. The result of this process is shown below in the morphological chart.

Function	Concept 1	Concept 2	Concept 3	Concept 4	Concept 5
Energy Extraction	Multiple Turbines in Parallel: Axis of rotation parallel to water flow	Multiple Turbines in Series: Axis of rotation parallel to water flow	Water Wheel with generator: Axis of rotation perpendicular to water flow		
Energy Transfer	Hydraulic pump and circuit	Direct Electricity generation	Air compressor	Water pump	
Energy Storage	Accumulator – Hydraulic pressure	Compressed air storage tank	Elevated water tank	Battery array (Lead Acid, Hydrogen Hybrid, or NiMH)	Direct electricity generation (No storage)
Energy Dissipation	Hydraulically-driven Generator	Air-driven tools or an air-driven generator	Gravity-fed hydroelectric generator	Direct Current connection to battery array	Heated Water

Table 1: Morphological Chart

The morphological chart shows all the different concepts for each component that we've mentioned. In the subsections below, we introduce a representative concept for each system component. The rest of the concepts are briefly explained in appendix A.

Energy Extraction: This component of the system will extract energy from the river's flow. Essentially, this component converts the kinetic energy of the water into some other form of energy that can be easily transferred to the camp without too much loss. As listed in the morphological chart, concepts for this component include: the hydroflow generator from MHL, multiple turbine blades used in parallel (see Figure 5), and a waterwheel. Figure 5 on the next page shows the concept for multiple turbine blades in parallel. This concept is similar to the hydroflow generator concept shown in Figure 4. However, in this concept, there will only be one turbine blade per turbine unit. This concept could allow us to add turbine blades to the system later on to increase the power extracted from the water. In this case, the power extracted from each turbine blade would add together after the power is converted into a form that will allow the summation of power. Since this summation of power is possible with pneumatic, hydraulic, and electrical circuits, selecting this concept will not limit our selection of concepts for other components of the system.

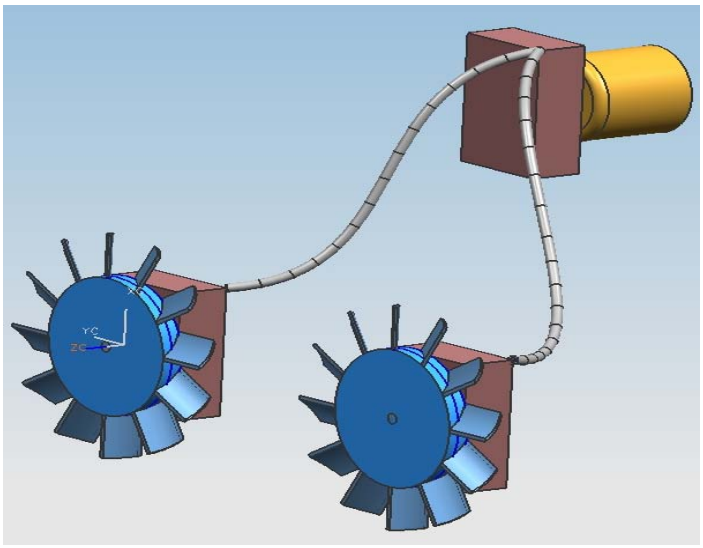

Figure 5: Multiple Turbine Blades in Parallel

Energy Transfer: The energy transfer component includes the energy conversion unit in the energy extraction unit and the circuit through which the energy is transferred. In the hydroflow generator in Figure 4, the energy conversion unit is located between the two blades and could either be an electrical generator or a hydraulic pump. As shown in the morphological chart, the concepts for the energy transfer component include: hydraulic pump/ circuit, electrical generator/ circuit, air compressor/ pneumatic circuit, and water pump/ flowing water. The energy transfer component of the system more or less determines the concepts required for many other components. For example, if the hydraulic pump/ circuit concept is selected, then the energy storage component will most likely have to be either a hydraulic accumulator or a battery array. In this case, the hydraulic pump converts the energy from the energy extraction component into a flow of pressurized hydraulic fluid. Then, the flow in the hydraulic circuit could cause energy to be stored as pressure in a hydraulic accumulator. Alternatively, the hydraulic circuit's flow could directly run a hydraulic generator, in which case the energy would have to be stored in a battery array, if energy storage is desired.

Energy Storage: As described in the previous section, concept selection for the energy storage component is strongly dependent on the concept selection for the energy transfer component. In fact, concept generation for these two components typically occurred simultaneously. A concept for the energy storage component typically comes with a required energy transfer concept. Therefore, one can see the relationship between the energy storage and energy transfer concepts in the morphological chart. These energy storage concepts include: hydraulic accumulator, battery array, compressed air storage tank, and elevated water tank. Here, the elevated water tank concept stores energy as the gravitational potential energy in water that's pumped up to a higher location. Wind generators in many places use this concept for storing wind energy. When the energy is needed, then the water is run down through a high head low flow hydroelectric generator, which is commercially available.

Energy Dissipation: This is the final component before useable electrical power is delivered to the research camp. The morphological chart shows that our concepts for this

component include: hydraulic generator, inverter, air driven tools or compressed air generator, heater/ water boiler, and a high-head/ low flow hydroelectric generator. If we ever intend to store energy in a battery array, the inverter mentioned here would be needed to convert the DC current from the battery to AC current, which is what the camp needs.

Concept Evaluation and Selection

After developing all the concepts for each component of the system, we began to reject inferior concepts so that we may ultimately arrive at the best final concept for the whole system. Since concepts for most components could be used together with multiple other concepts for another component, we did not directly narrow down the number of concepts for the whole system. Rather, we focused on rejecting individual concepts for each component of the system. For rejecting these concepts, we utilized a Pugh chart. The Pugh charts shown in appendix C depict our evaluation of each concept for each component. By using the Pugh charts and other research information, we eliminated the concepts that are crossed out in the revised morphological chart below.

Function	Concept 1	Concept 2	Concept 3	Concept 4	Concept 5
Energy Extraction	Multiple Turbines in Parallel: Axis of rotation parallel to water flow	Multiple Turbines in Series: Axis of rotation parallel to water flow	Water Wheel with generator: Axis of rotation perpendicular to water flow		
Energy Transfer	Hydraulic pump/ circuit	Electrical generator/ circuit	Air compressor	Water pump	
Energy Storage	Accumulator – Hydraulic pressure	Compressed air storage tank	Elevated water tank	Battery array (Lead Acid, Hydrogen Hybrid, or NiMH)	Direct electricity generation (No storage)
Energy Dissipation	Hydraulically-driven Generator	Air-driven tools or an air-driven generator	Gravity-fed hydroelectric generator	Direct Current connection to battery array	Heated Water

Table 2: Revised Morphological Chart

Below is a list of all the rejected concepts and a brief description of why they were rejected.

Energy Extraction

1) Water wheel with generator: After doing some research on waterwheels, we determined that the typical waterwheel would be too massive, and too difficult to setup. Since our system must be portable, the waterwheel concept is not suitable. Also, research showed that waterwheels are most efficient when the river has a low flow rate and high head [2]. Since we will have a high flow rate with low head, turbine blades are more suitable.

2) Multiple turbines in parallel: After running a few tests in MHL's testing basin, we realized that the force from the flow causes problems in trying to secure the energy extraction component of the system. Since this concept requires securing multiple separate components, we decided that using the multiple turbines in series would be preferable. Placing the turbines in series would require securing half as many underwater components as if the turbines were places in parallel.

Energy Transfer

1) Air compressor: From correspondence with Dr. David Swain at the National Vehicle Fuel and Emissions Laboratory of the Environmental Protection Agency, we determined that using a pneumatic circuit with and air compressor would be less efficient than using hydraulic or electric circuits. This is because of the significant turbulence losses in the air that wouldn't be as big of a problem in hydraulic or electric circuits.
2) Water pump: See explanation for the rejection of the elevated water tank concept in the Energy Storage section below. We rejected this concept because it requires energy storage by an elevated water tank.
3) Hydraulic pump/ circuit: Dr. David Swain of EPA has informed us that the low temperatures in the Alaskan environment would necessitate the use of special hydraulic fluid that would maintain its viscosity at lower temperatures. Moreover, due to environmental concerns, the hydraulic oil we would need to use must not pollute the environment if it happens to spill. Based on these concerns, we have decided that the electrical circuit may be a better concept to use.

Energy Storage

1) Hydraulic accumulator: Along with the problem of needing special hydraulic fluid, Dr. David Swain has also point out that the hydraulic accumulator needed for our energy storage requirements would be much too heavy to be part of a portable system. Therefore, we have determined that other storage methods would be more suitable for our application.
2) Compressed air storage tank: See explanation for air compressor in the Energy transfer section. Pneumatic components are all rejected because of inefficiency due to turbulence losses.
3) Elevated water tank: Some simple calculations showed that any water tank that can hold any significant amount of energy would be too large for our purposes. For example, if we want 8 kilowatt-hours of energy, which is equal to 28.8 Mega joules, with a water tank at 8 meters high, then the volume of the tank can be determined with the equation:

$$V = \frac{Energy}{Density \times Height \times grav.\_const.} \quad \text{Eq. 1}$$

Using this equation, we determined that the necessary volume would be 367 m^3. If the tank were a cube then each side of this tank would be 7.2 meters long. This conservative calculation does not even take frictional losses in the pipe into account, and the tank would already be too large to transfer with a bush plane. Because of this, we rejected all the concepts that require using an elevated water tank as the energy storage component.

Energy Dissipation

1) Air driven tools or an air driven generator: See explanation for the air compressor in the Energy transfer section. This energy dissipation concept requires a pneumatic circuit, which we have already rejected.
2) Gravity-fed hydroelectric generator: See explanation for the elevated water tank concept in the Energy storage section. This energy dissipation method required using an elevated water tank, which we have already rejected.

Engineering Analysis

Initially, we used an energy equation to help us determine an approximate amount of power that is available in the river flow. Then, using a control volume analysis, we determined an ideal approximation of the amount of energy that our blades should be able to extract. Afterwards, we used the linear momentum equation to predict the force of the flow on our system. Finally, by using the force on the unit, we determined the stresses on the bars connecting the sealing and the outer casing. The details of these analyses are described below.

Total Energy in Flow

An equation for the total energy in a fluid flow is:

$$\frac{P}{\rho} + \frac{V^2}{2} + gz + \hat{u} = e \qquad \text{Eq. 2}$$

Where P is the pressure, ρ is the water's density, V is the water velocity, g is the gravitational constant, z is the height with respect to the reference state, û is a term related to the internal energy of the water, and e is the specific total energy [2]. Since the turbine blades are only able to extract kinetic energy from the flow, the energy available for extraction via the turbine blade is just:

$$\frac{V^2}{2} = e_{Turb} \qquad \text{Eq. 3}$$

If we multiply equation 3 by the water mass flow rate, then we get:

$$\frac{\dot{m}V^2}{2} = \dot{W} \qquad \text{Eq. 4}$$

Where $\dot{m}$ is the water mass flow rate, and $\dot{W}$ is the power available for extraction by the turbine blades. Since the water mass flow rate is equal to the product of the density of water with the cross sectional area and the velocity, we can determine the amount of power available for turbine extraction for any given pair of cross sectional area and water velocity value. Using this equation, we calculated the total energy in an area equal to the size of the turbine blades for a variety of water speeds (see appendix E). From this data we've determined that one single hydroflow generator unit would not be able to supply the 10 kW of power for the research camp. However, using multiple hydroflow generators together could allow us to produce enough power for the camp.

Control Volume Analysis

The theoretical shaft power is based on linear momentum equations for turbines seen below in equations 5 and 6.

$$w_{shaft} = U_2 V_{\theta 2} - U_1 V_{\theta 1} \qquad \text{Eq. 5}$$

$$P_{shaft} = \dot{m} w_{shaft} \qquad \text{Eq. 6}$$

V is the absolute velocity of the water, W is the velocity relative to the moving blade, and U is the velocity of the blade, they are defined in Eqs. 7 and 8 as well as Figures 7 and 8 seen below:

$$\vec{V} = \vec{V}_\theta + \vec{V}_x \qquad \text{Eq. 7}$$

$$\vec{V} = \vec{U} + \vec{W} \qquad \text{Eq. 8}$$

Using equations 5 through 8 with the control volume defined below in Figure 6 we were able to calculate the theoretical shaft power for a variety of blade angles which is displayed in Graph 1. This figure shows that an increase in blade pitch angle leads to an increase in shaft power. Shaft power is also shown to increase with an increase in the water velocity. Based on these findings were able to predict that our blade with the largest pitch angle would extract the most power from the water which is consistent with our results in the testing section.

This analysis was based on the following assumptions:

1) The entry control surface is equal in area to the exit control surface so $V_1 = V_2$

2) $\vec{U}_1 = \vec{U}_2$ i.e. the blade spins at the same speed on both points

3) There is no flow in the radial direction

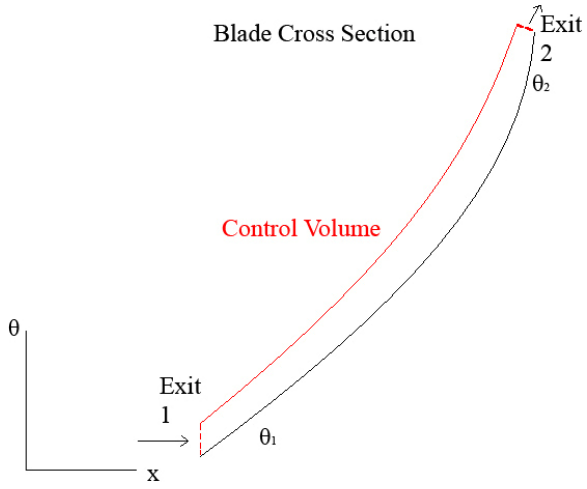

Figure 6: Blade control Volume

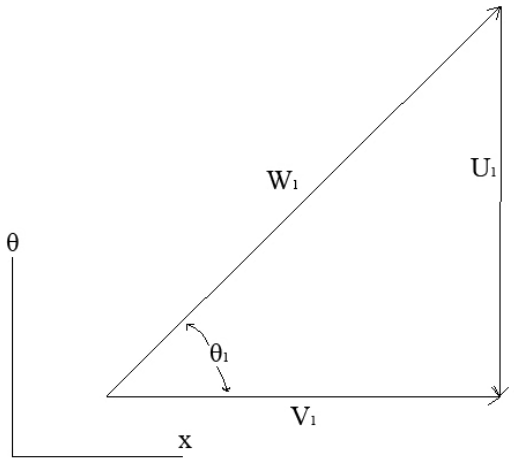

Figure 7: Entry Velocity Triangle (1)

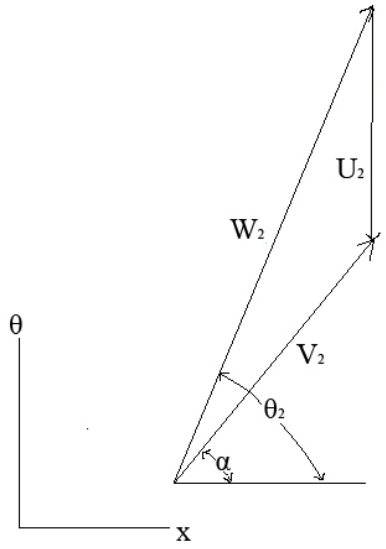

Figure 8: Exit Velocity Triangle (2)

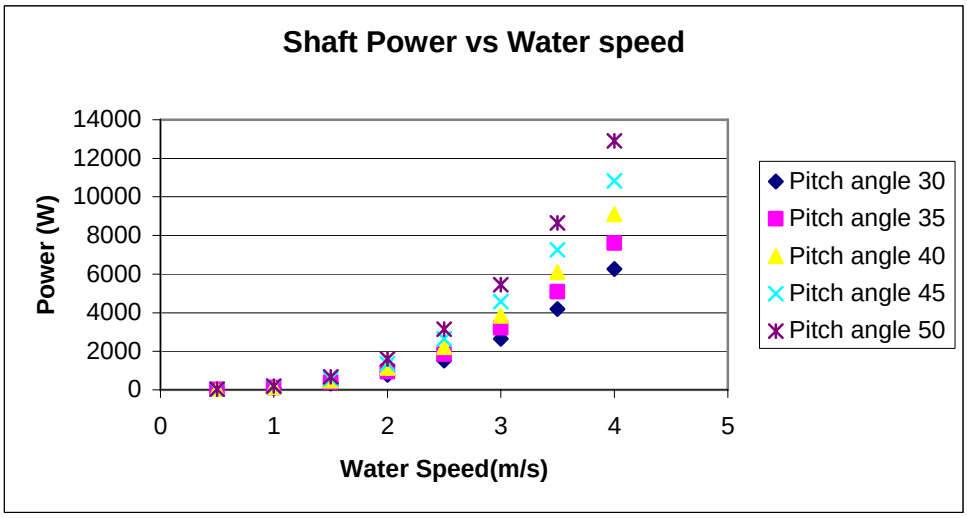

Graph 1: Power Output Increase with Pitch Angle

Anchoring Force Calculation

To help MHL determine a way for securing the hydroflow generator, we have calculated the amount of force that the flow would exert on the hydroflow generator. This analysis required the linear momentum equation [2]:

$$\frac{\partial}{\partial t}\int_{CV} V\rho dV + \int_{CS} V\rho V \cdot \hat{n} dA = \sum F_{Contents\_of\_CV} \qquad \text{Eq. 9}$$

Where n is a unit vector normal to the control surface facing away from the control volume, A is for the cross sectional area of the flow, and F is for the force. Since we don't expect the velocity to suddenly change, we assume a steady flow. With this assumption, the time differential term integrating through the control volume is now 0, since we assume that there will be no change with respect to time. Since we know the flow velocity and flow cross sectional areas, and the density of water we can calculate the

left hand side of this equation and thereby determine the force on our system. We performed this analysis on both the nose cone and the blades to determine the force on each of those components. The result of this analysis is shown below in Graph 2. Note, however, that we neglected the surface drag on the unit. Therefore, the actual force should be slightly greater than what we have predicted.

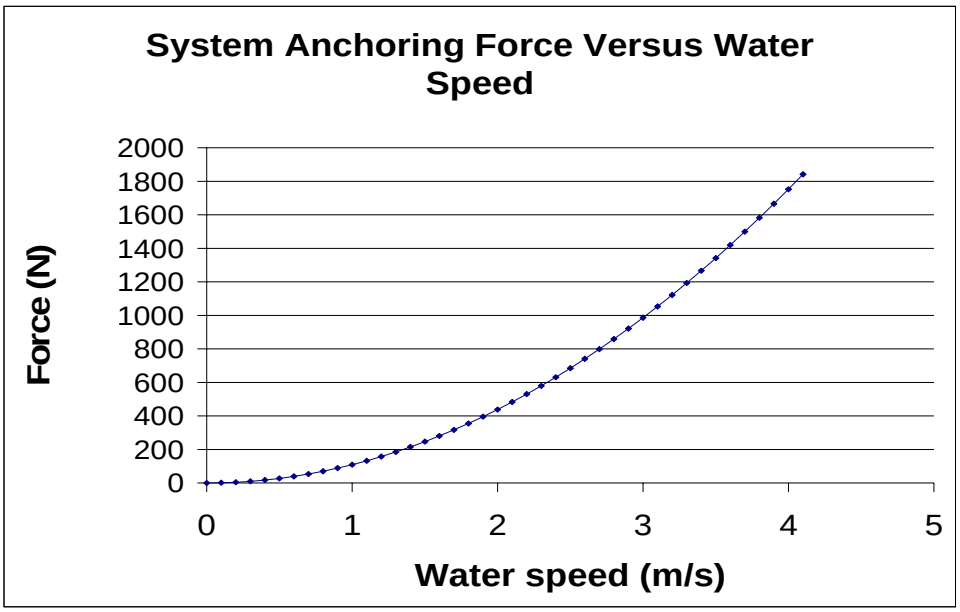

Graph 2: System Anchoring Force Versus Water Speed

Using this graph, MHL could determine the most suitable method for securing the hydroflow generator such that the forces do not overwhelm the anchoring system.

Connecting Rod Bending Stress Analysis

Using the forces from the previous analysis, we performed a bending stress analysis on the rods connecting the outer casing and the sealing. For this analysis, we used the force on the system at the worse case of the unit's operation: 4 m/s. Since we have 12 connecting rods, if we assume that the force is evenly distributed among the 12, then each rod will experience $1/12^{th}$ of the force, which is 146 Newtons. Then, modeling each rod as a cantilever beam, we determined that the maximum bending moment, M_{max}, is 52.5 N·M. Using the bending stress equation with the equation for the moment of inertia, I:

$$\sigma_{Bending} = \frac{M_{\max} \cdot r}{I} \qquad \text{Eq. 10} \qquad\qquad I = \frac{\pi \cdot r^4}{4} \qquad \text{Eq. 11}$$

Where r is the radius of the rods, we've determined that the maximum stress that the rods could experience is 132.8 Mpa. Since our rods have yield strengths of 434 Mpa, our design here has a safety factor of 3.27. We feel that this kind of safety factor may be necessary because of the unpredictable and harsh operating environment. Moreover, this safety factor will take care of various simplifications and assumptions we have previously made in our analyses. Graph 3 shows a plot of the rod bending stresses at varying velocities.

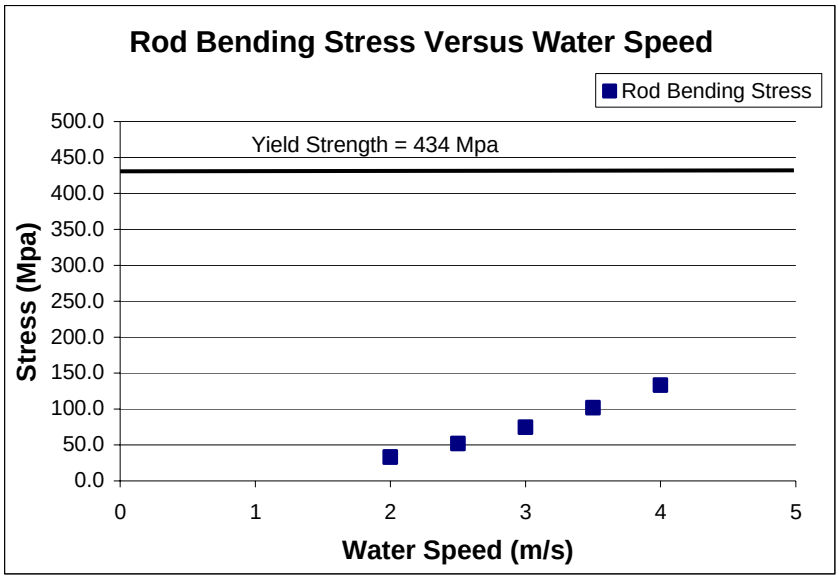

Graph 3: Rod Bending Stress Versus Water Speed

As shown in this graph, our design for the connecting rods is safe for the given operation conditions.

Final Design

Our final design for the hydroflow generator uses two turbine blades connected in series: one after another. The CAD drawing of the final design is shown in Figure 9 below.

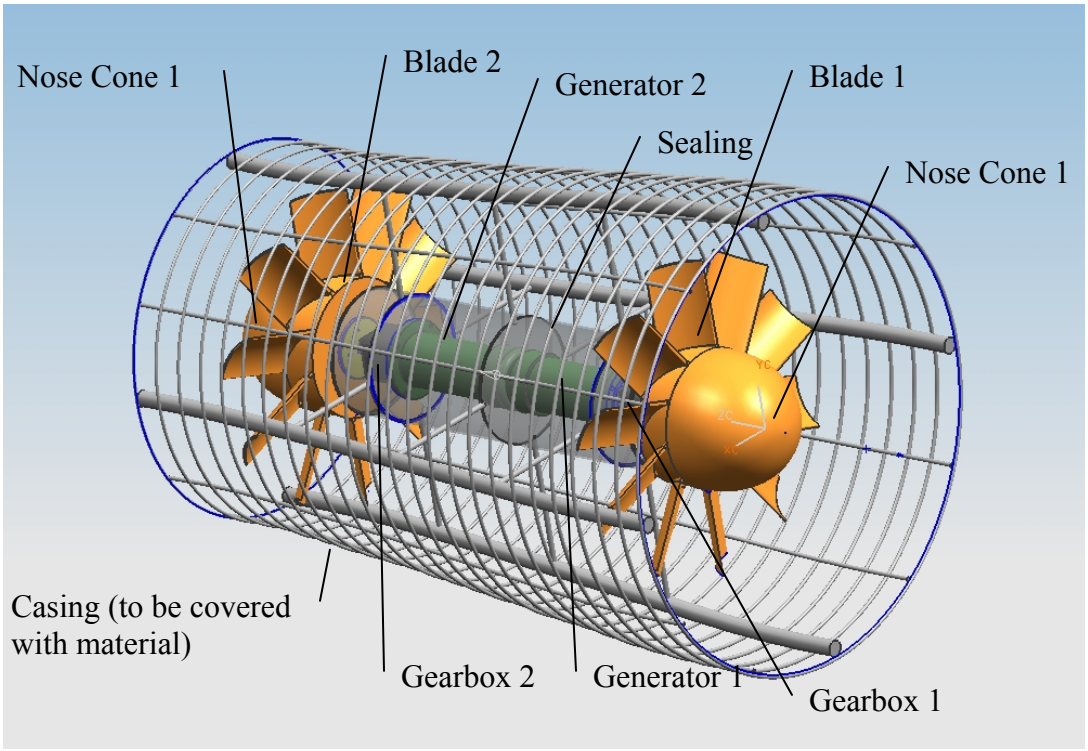

Figure 9: Hydroflow Generator CAD Drawing

The left and front view of the CAD drawing of the unit is included in appendix G. As depicted in Figure 9, the heart of the hydroflow generator is described by the following outline:

Nose cone 1 → Blade 1 → Gearbox 1 → Generator 1 → Blade 2 → Gearbox 2 → Generator 2 → Nose cone 2.

In this setup, the first nose cone would separate the water, which would then spin blade 1. The spinning of blade 1 would be transmitted through the first gearbox so that the generator would be driven with the appropriate torque and RPM. According to our calculations, both of the gearboxes will need to have a gearing ratio of 9:1. Not shown in Figure 9 is the electrical line that would be coming out from the generator to carry the power to the shore. After the water flows past the first blade, it will smoothly flow over the sealing, which keeps the water out of the electrical components. Past the sealing, the water will flow through the second blade, which would drive the second generator, just as how the first blade drives the first generator. Since the blades are optimized when receiving flow from a certain direction, both blades will face the same direction, even though the nose cones will face the opposite directions. Note that the two generators and blades are on separate shafts so that rotation at different speeds will not be a problem for the unit. Once the flow proceeds through the second blade, the second nose cone will help decrease the amount of turbulence. The whole internal hydroflow generator system, along with the blades, will be covered and protected by an outer casing.

The sealing for the generators and gearboxes would be filled with special low viscosity non-conducting oil to help decrease the pressure difference across the sealing and prevent water from seeping in through the seal. Although it seems that the oil could introduce losses by resisting the spinning of the gears and the generator components, researchers at MHL, who have extensive experience regarding this subject, affirms that the losses would not be significant, due to the oil's low viscosity. For securing the entire hydroflow generator unit, 12 steel rods would connect the sealing to the outer casing, which would then be secured to whatever anchoring mechanism is required. The design of the specific anchoring mechanism would depend on the unit's immediate environment. Since the anchoring mechanism is outside of the scope of our task, we will not discuss this mechanism in detail.

Apart from protecting the internal components of the unit, the outer casing could be used to help increase the flow velocity. As shown in the dimensioned figures in appendices G and H, the entrance of the outer casing has a larger diameter than the exit. The principle behind this feature is like that of a nozzle, which should ultimately increase the flow velocity. The problem with applying a nozzle feature to the outer casing, however, is that the casing is open to the flow so that the pressure at the entrance and exit of the casing is the same. Since decreasing the diameter of the exit of the casing would increase the pressure in the casing, this pressure difference between the inside of the casing and the entrance of the casing would "push" back against the flow and thereby decrease the flow. This argument describes how decreasing the diameter for the sake of increasing the flow speed could backfire and result in decreased flow. To determine the optimal amount of decrease in the diameter between the entrance and the exit, computational fluids analysis

or further testing may be required. But further research into this feature of the system could result in increased power output.

At the heart of the system, the main mechanism for extracting the power is in the generator. This component converts the rotational work of the shaft into electrical power. This conversion happens through the phenomena of electromagnetic induction. When a conductor is moved through a magnetic field, a current is induced. For our generator, the conductor is a large coil of conducting wire, and the magnetic field is produced by permanent magnets in the generator. When the input shaft of the generator in rotated, the conducting coils move through the magnetic field and a current is induced in the coils. The force resisting the rotation of the shaft is determined by the load of the generator, so that if more power is being drawn, a greater force will resist the input shaft's rotation.

The dimensions of the whole system were mainly determined by the blades that MHL provided to us. The dimensions for the blades are included in appendix D, and the dimensioned CAD drawings are included in appendices G and H. Increasing the diameter of the blades and the casing would result in increased power extraction, since more flow is available to provide torque to the blades. However, increasing the diameter of the blades and casing will clearly increase the unit's weight and bulk, thereby decreasing its portability. Depending on the power and portability requirements, the hydroflow generator could be altered to suit the needs of the particular circumstance.

Prototype Test Plan

Testing of the prototypes was carried out in two stages. The purpose of the initial stage was to get a rough measurement of the amount of energy that could be captured by the blades. For the second stage of testing, we used the information gained from the first round of testing to make the proper generator and gearing selections. We then ran the two different blades through the test basin while taking actual measurements of the amount of energy produced by the generator.

Initial Turbine Blade Testing

We performed tests on our two turbine blades at MHL's testing basin. In their testing basin, a movable carriage on a track that runs the length of the basin is setup to run across the top of the basin at user specified speeds. By fastening the testing apparatus with the turbine blade onto the carriage, we simulated a certain water flow speed by moving the dynamometer at that exact speed. For these tests, technicians at MHL helped us setup our testing apparatus.

A labeled picture with the test apparatus is shown below in Figure 10. When the cart is moving, the apparatus is brought through the water at the desired speed. This causes the turbine blade to spin. The spinning of the turbine blade is then transmitted through a bevel gear to become rotation in the shaft that's behind the flow separator. The flow separator here decreases the apparatus's resistance as it moves through the water. To measure the angular velocity of the blade, a spur gear is built into the shaft so that the magnetic encoder in the apparatus could read the velocity by the rotation of the gear. To measure the torque associated with the turbine blade's rotation, we used a pneumatic clutch along with a force gauge. We used the pressure dial to set the pressure in the

pneumatic clutch. This pressure then causes another metal cylindrical device to turn. This device has an arm that then presses down on the force gauge. Using the force readings and the length of the arm, we could then determine the blade's torque in ft*lbs using equation 12 below, where Force is the force measured on the load cell, (1/3) is the length of the moment arm in feet, and 2 is the gear ratio for the bevel gear.

$$Torque = Force * \left(\frac{1}{3}\right) * 2 \qquad \text{Eq. 12}$$

During testing, we broke a gear box because the torque was too great for the gear box. Because of this, we had to be careful in the rest of our tests to keep the clutch pressure and the overall cart speed low enough to keep the torque within the acceptable range of the bevel gear.

Also, at high speeds, the magnetic encoder began reading incorrect values, despite our use of a flow separator. This was due to the backwards bending of the shaft below its mounting point causing the portion of the shaft above its mounting point to bend forward. This forward motion was large enough to cause a collision between the magnetic encoder and the gear it was reading the rotational speed from.

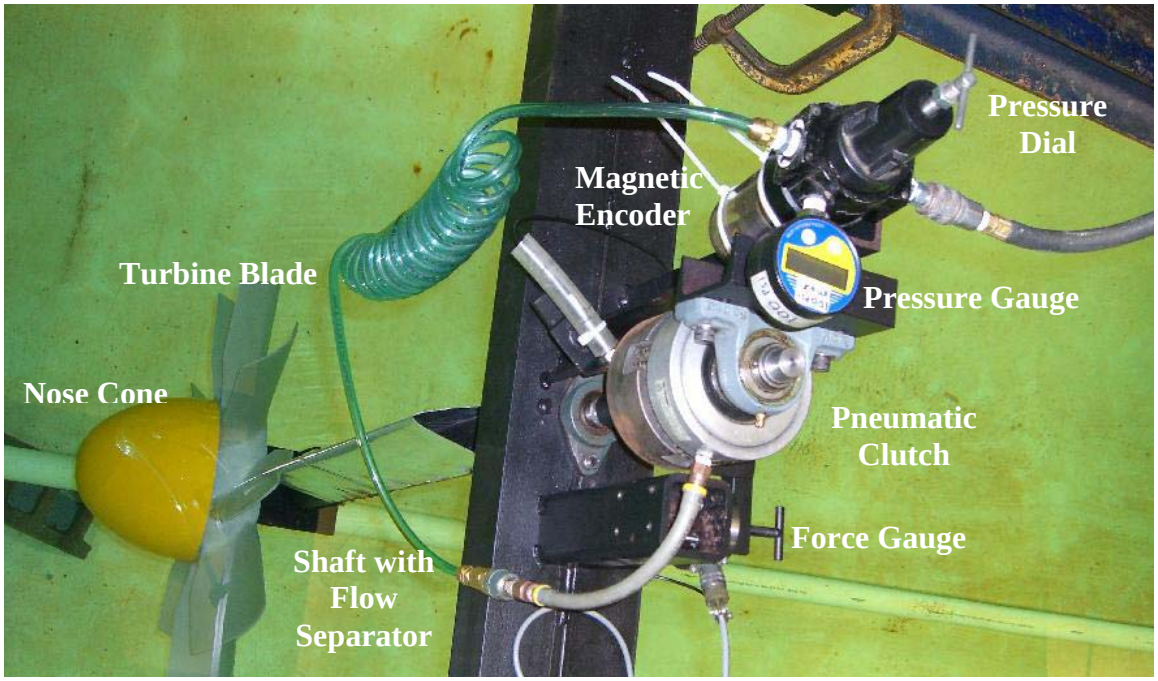

Figure 10: Turbine Blade Test Apparatus

To determine the performance of the blade at different conditions, we varied the pneumatic clutch's pressure and the water speed while recording the blade's angular velocity. The magnitude of the pressure in the clutch simulates different loads that would be placed on the electric generator. Although in application we won't be able to control the water speed, testing different water speeds allowed us to develop a better understanding of the power extraction system so that we may extrapolate from our data to predict system behaviors at water speeds that we were unable to test.

In our testing, we used two different turbine blades: one with a slightly smaller diameter and lower pitch angle, and another with a larger diameter and higher pitch angle. A summary of the test data and blade characteristics is included in appendix D. In our analysis, we ran a few tests with no pressure in the clutch in order to determine the amount of frictional loss in the system. This loss was then incorporated into our calculation for the torque. Using the torque and the speed, we determined the power by the relation:

$$Power = Torque \times Angular\ Velocity \quad \text{Eq. 13}$$

Graph 4 on the next page is the power versus speed curve for the second blade that we tested, which is smaller with a lower pitch angle. The smaller blade was chosen for representative values and future decision making criteria due to its higher calculated power output. In order to help interpolate and extrapolate the data at speeds that we have not tested, we fitted curves to our data. By maximizing the R^2 values, we determined that a binomial curve results in the best-fitting curve. Even though we were not able to test at water speeds of 4 m/s, the high R^2 values from our curves suggest that extrapolated estimates should be somewhat reliable.

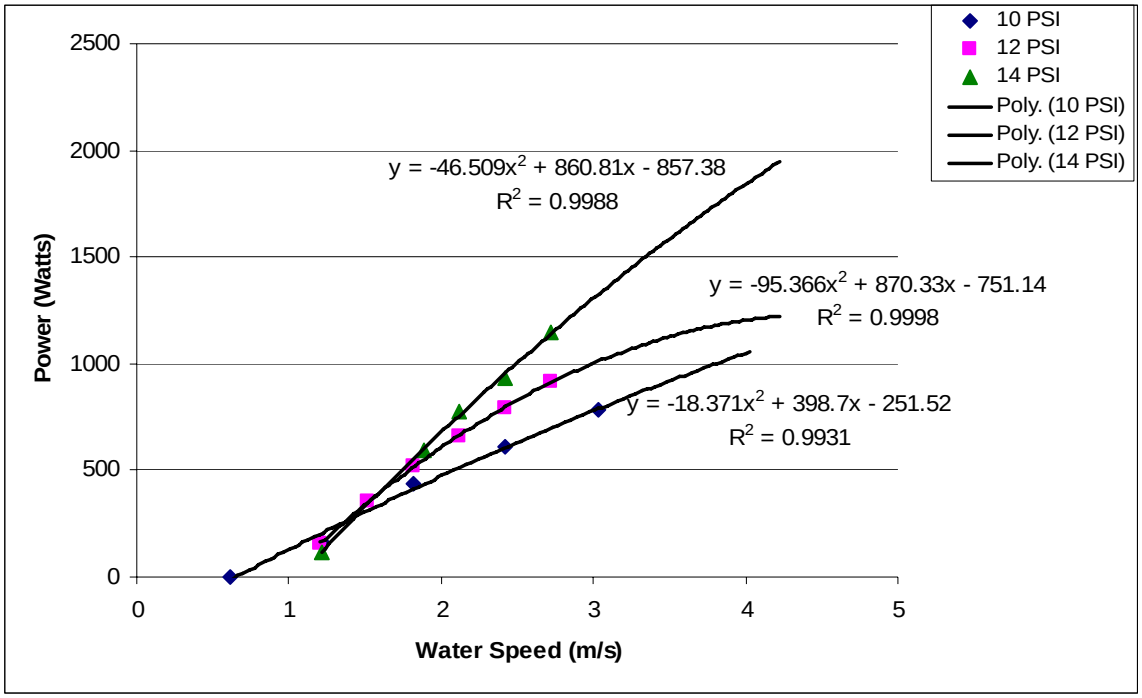

Graph 4: Power – Speed Curve for Blade 2 (Smaller Blade)

As predicted in equation 13, we see in Graph 4 that the power increases with the water speed. Also, at the range of water speeds that we will operate at, 2 to 4 meters per second, increased load results in increased power. To further aid our predictions of the blade characteristics at speeds and loads that we have not tested at, we completed a regression analysis and determined this relation between our variables:

$$Power = 936 - 818 \times Speed - 0.0127 \times Load + 0.0108 \times Speed \times Load + 30.1 \quad \text{Eq. 14}$$

Where Power is in W, Speed is in m/s, and Load is in N/m^2. Using this equation, we could roughly estimate the expected power with a given speed and load.

Design Optimization Based on Test Data – Generator Selection

We then selected the generator to be used in our second prototype based on the test data summarized in Graph 4**.** The first step in selecting the generator was to find a design that was optimized for high efficiency use at various speeds and levels of power output. To solve this problem, we looked at generators traditionally used in wind power applications, as this represents an extreme example of the conditions our generator will be subject to. Researchers at MHL have previously used generators from windstreampower.com for lower power research applications, so that served as a starting point in our decision making.

After locating a supplier with generators optimized for our application, the next task was to select the proper size generator based on the estimated power output from our first round of testing. After talking to a sales representative from windstreampower.com, we learned that their generators have the same level of efficiency at very low power outputs as they do at higher levels. This made the deciding factor in our selection the maximum power output that the generator could produce.

We then estimated the maximum power that could be produced using the equation fit to the data points representing our maximum resistance of 14 psi on Graph 4 at a maximum water speed of 4 m/s, equation 15 below.

$$Power = -46.509 * v^2 + 860.81 * v - 857.38 \quad \text{Eq. 15}$$

This gave us a maximum power of 1841 Watts. Due to errors in the initial test setup, we knew this value to be only a rough approximation. Given that this value is an approximation and that all generators offered by this company are very efficient at lower speeds and power outputs, we selected a generator with a maximum power output of 2700 Watts, model #443905, 30 Amp Permanent Magnet DC Generator from windstreampower.com.

We then used the characteristics of our selected generator, shown in Appendix J, as well as our angular velocity and torque measurements from our initial test to select the proper gearing ratio. Based on our initial data, at 2 m/s we achieved a rpm range of about 120 to 200 rpm. At a 9:1 ratio, this would give us generator shaft speeds of 1080 to 1800 rpm. For faster flow rates, we selected a 6:1 gear ratio to be used for testing.

Second Prototype Testing

With all of the information gained during the first round of testing, we were able to greatly improve our method of measuring energy extracted from the flow as well as employing a chained gear setup which is much closer to what is to be used in the final design.

The physical frame that held the blade in place while the carriage moved forward through the tank remained unchanged, as it is to a large extent dictated by the setup of the carriage and the depth at which it must hold the blade to achieve accurate test results. However, instead of a bevel gear, we now used a shaft held in place by two roller bearings mounted to a flat steel plate welded the bottom of the steel pipe that extends into the tank. A 72 tooth gear is attached to the end of the shaft opposite the blade to transfer the mechanical rotation of the blade to the test rig by means of a chain.

The chain extends up out of the water and connects to a smaller 8 or 12 tooth gear that is supported by another roller bearing and connected to the shaft of the generator. In this manner we could directly measure the voltage being produced by the generator by attaching a special resistor made for high power applications to the generator leads to simulate the load of charging an array of batteries. We used a standard digital multi-meter applied at the leads to measure the voltage being produced at different carriage speeds. The power produced for each run was then calculated from the relationship shown in equation 16 below.

$$Power = \frac{V^2}{R} \quad \text{Eq. 16}$$

The results obtained from this round of testing are summarized in the graph of power output vs. carriage speed for various resistive loadings shown below as well as in Appendix B.

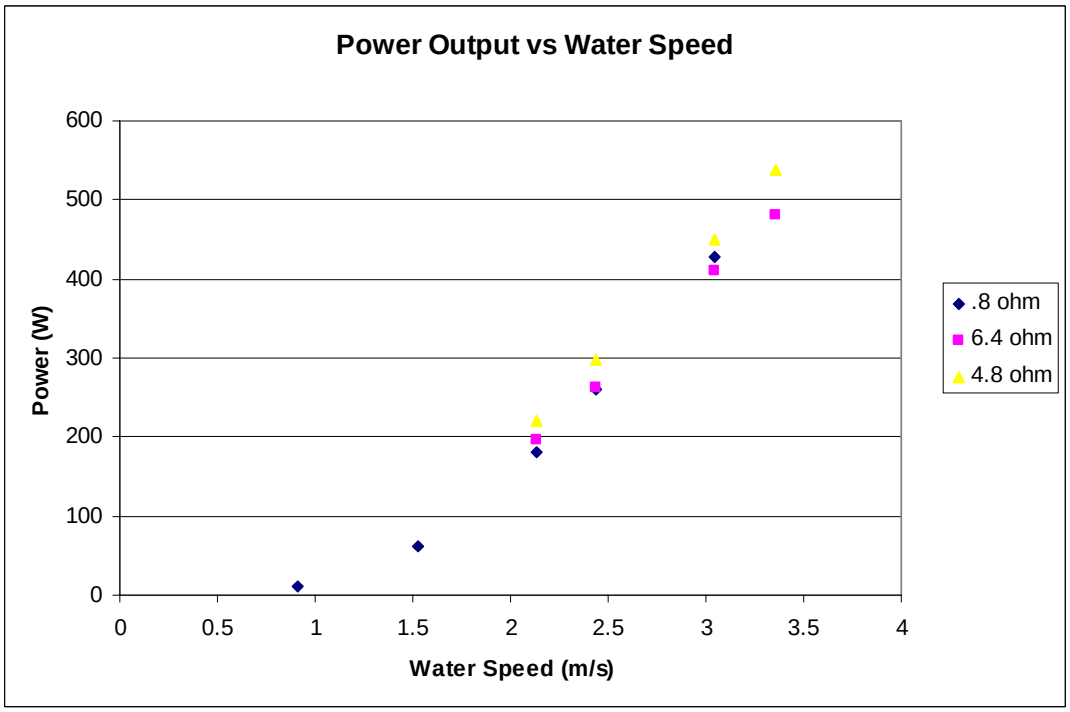

Graph 5: Prototype Power Output Versus Water Speed

Sources of Error
As can be seen from the graph, the amount of power measured at the leads of the generator is significantly less than was predicted in the previous round of testing. There are several possible explanations for this. While the measuring the power produced directly at the generator is much more accurate than producing an approximation based on the rotational force produced by friction from an pneumatic clutch, it is still only measuring the amount of power that actually reaches the surface of the test carriage. A single bevel gear, encased in a protective housing, is a much less error prone method of transferring mechanical power than a chain with spur gears.

The problem in predicting the error that the spur gear/chain setup introduces into our results is that it is different at different speeds. There are two reasons for this. The first is that the drag force that the water exerts on the chain is proportional to the chains horizontal and vertical speed through the water. The second reason is that, due to bending in the mechanical support structure for the blade, the tension in the chain is not constant. As the carriage pushes the blade through the water, in addition to rotating it, it is also pushing in directly backwards. The force is enough to provide a significant displacement of the blade relative to the carriage. The chain is forced into a position of greater tension and friction to try and accommodate this new blade position.

Comparison to Theoretical Values
Throughout the course of this project, we have always been aware that there are several large sources of inefficiency in the model we are using to test this concept. The blades are from an old semi, and are optimized to drive air over a radiator, not be driven by water in a river. This aspect of the project alone, if optimized, could greatly improve the amount of energy procured. In addition, any of the methods we used to transfer the mechanical power from the water were at best 80% efficient; in practice they were probably much worse. In practice, direct shaft coupling with a single spur gear would provide better power transfer. Therefore although the values obtained from the second round of testing are nearly an order of magnitude less than the values obtained through our theoretical analysis, the important part is that they follow roughly the same functional form as the theoretical values. This verifies the validity of our calculations, and provides a basis for further research into the optimization of this concept.

Prototype Manufacturing

The construction of our test rig can be broken down into two areas, component procurement and assembly. Due to the nature of our project, many of the components could be bought, with no modifications required for assembly. We have already ordered two generator heads, each of which will be connected to a turbine blade. We have procured sprockets of 9:1 and 6:1 ratios in combination with steel roller chain 41 with ½ inch pitch and 0.306 inch width that will be needed for matching the turbine blade's rotation to the optimal speed and torque for the generator head. We have additionally procured and installed roller bearings (two 5/8 inch shaft size bearings for the generators and four ¾ inch shaft size bearings for the turbine blades) that will help connect and support the shaft of the two blades as well as the shafts turning the generators.

The other components were fabricated by the technicians at MHL. The hubs used to mount the turbine blades to their respective shafts were made by cutting raw ¼ inch thick steel into circular shapes using an electrically driven diamond-dusted blade and then smoothed on a lathe. Holes for mounting were drilled into the disks and the lathed shaft portion was welded on. The frame to support the turbine blades as well as the generators and casing is composed of 2 inch schedule 40 steel piping welded to a 2 inch by 2 inch angle iron of ¼ inch thickness. To weld these components together, a metal inert gas welder was used with an internal metal feed system.

Figure 11: Blade to driveshaft coupler

The nose cone was also manufactured on site. It was constructed from a wooden center that was surrounded with shaped foam. The foam was glued to the wooden middle section and a fiberglass shell was installed on top of the foam, creating a light but strong exterior.

Final Design Manufacturing

Generator Sealing

The most complicated aspect of the manufacturing of the final design is the watertight generator housing. The outer casing of the housing will be made from steel piping, sealed with rubber gaskets. The major protection from leakage will come from a special low viscosity non-conducting liquid that the generator assembly will be submerged in within the housing. This will eliminate a pressure differential between the inside and outside of the casing and thereby greatly reduce the chances of the generator being exposed to water.

Gearing

The final design would use a gearbox that provides a 9:1 constant gear ratio and could be purchased in a ready to use form from McMaster-Carr industrial suppliers. This gearbox would fit completely behind the nosecone as pictured in the CAD drawing.

Outer Casing

The design's casing will decrease in cross sectional area in order to accelerate the flow and thereby increase the power output. The casing would be composed of a cage of tubes as seen in Figure 9 on page 14. This cage will then be wrapped with fiberglass.

The material that the inside rib cage is composed of can vary depending on function. As it is designed here, the frame for the casing can be constructed of plastic or light wood, as the fiberglass coating will provide all of the strength necessary for flow restriction. If however, a design were needed that would be able to sustain a hit from an iceberg or from a rock being pushed along the bottom of the river, the casing could then be manufactured from steel bars that would provide the necessary amount or structural stability.

In order to manufacture the casing, thin plastic rods could be slightly heated and then bent into the required shape, where they could be tied together with wire. Then fiberglass could be soaked with epoxy and then applied over the outer casing. Once this epoxy hardened the plastic inner skeleton could be removed.

Bill of Materials

For our prototype, we have generated an estimated bill of materials and a cost estimation analysis. The bill of materials is presented as Figure 12. A separate bill of materials for the final design, which was not fabricated, is shown in Figure 13.

Quantity	Part Description	Purchased From	Part Number	Price (each)
1	8 Tooth Sprocket for 41 Steel Chain with 1/2" Pitch	McMaster*	2737T93	$6.04
1	12 Tooth Sprocket for 41 Steel Chain with 1/2" Pitch	McMaster*	6280K502	$8.74
2	72 Tooth Sprocket for 41 Steel Chain with 1/2" Pitch	McMaster*	2737T737	$35.31
1	50' 41 Steel Roller Chain 1/2" Pitch 0.306" Dia.	McMaster*	6261K25	$132.50
3	10' 2" x 2" Angle Iron	McMaster*	8968K636	$65.51
4	3/4" Shaft Size Roller Bearing	McMaster*	6384K79	$10.35
2	5/8" Shaft Size Roller Bearing	McMaster*	6384K76	$7.98
1	2" Schedule 40 Steel Pipe 60" Length	McMaster*	7750K236	$49.93
2	5/8" Dia. Unhardened Precision Steel Drive Shaft 24"	McMaster*	1346K25	$15.77
2	3/4" Dia. Unhardened Precision Steel Drive Shaft 24"	McMaster*	1346K32	$20.05
2	30A Permanent Magnet DC Generator (+ Shipping)	Windstream Power LLC**	443905	$789.00
2	Full Wave Bridge Power-Up Diode Kit	Windstream Power LLC**	272125	$22.00
2	8" Diameter Mounting Disk	University of Michigan		$0.00
1	Housing Barrel	University of Michigan		$0.00
1	50 ft 12 Guage DC Wire	University of Michigan		$0.00
1	Wooden Nose Cone	University of Michigan		$0.00
1	Fiberglass Tail Cone	University of Michigan		$0.00
1	1/8" Thick Galvanized Steel Sheet Metal 6" x 10'	University of Michigan		$0.00

*http://www.mcmaster.com
**http://www.windstreampower.com

Total = $2,200.58

Figure 12: Bill of Materials for Prototype

Quantity	Part Description	Purchased From	Part Number	Price (each)
2	Parallel Shaft Spur Gear 3.9:1 Ratio	McMaster*	6481K74	$203.13
3	10' 2" x 2" Angle Iron	McMaster*	8968K636	$65.51
4	3/4" Shaft Size Roller Bearing	McMaster*	6384K79	$10.35
1	2" Schedule 40 Steel Pipe 60" Length	McMaster*	7750K236	$49.93
4	3/4" Dia. Unhardened Precision Steel Drive Shaft 24"	McMaster*	1346K32	$20.05
30	6' Low Carbon Steel Rod 1/8" D Alloy ASTM 1018	McMaster*	8920K11	$3.49
3	5/8" Diameter rods of ASTM A108 Steel with 6' length	McMaster*	6673T226	$28.50
2	30A Permanent Magnet DC Generator (+ Shipping)	Windstream Power LLC**	443905	$789.00
2	Full Wave Bridge Power-Up Diode Kit	Windstream Power LLC**	272125	$22.00
1	Wooden Nose Cone	University of Michigan		$0.00
1	Fiberglass Tail Cone	University of Michigan		$0.00
2	8" Diameter Mounting Disk	University of Michigan		$0.00
50	Sheet Metal Screw	University of Michigan		$0.00
1	50 ft 12 Guage DC Wire	University of Michigan		$0.00
1	Sheet of 5 m^2 of fiberglass	University of Michigan		$0.00

*http://www.mcmaster.com Total = $2,586.52
**http://www.windstreampower.com

Figure 13: Bill of Materials for Actual Design (Not Prototype)

Using the bill of materials along with estimated labor costs, we have developed a cost estimate. The total cost of raw materials and parts is $2,200.58 for the prototype and $2,586.52 for the final design. There are two primary sources of labor: the cost of welding and the cost of assembly/bending. The cost of welding is estimated to cost $45 per hour and require 10 hours using two people, resulting in a cost of $900. The assembly/bending are estimated to cost $45 per hour and require 30 hours using two people, resulting in a cost of $2700. This results in a net cost of labor of $3600 and an overall net cost for the prototype and final design of $5,800.58 and $6,186.52, respectively. Note that for our estimation, certain materials used are provided by MHL. These materials are free for our team to use, so their cost is not included in the cost estimate.

Discussion for Future Improvements

Due to the limited amount of time that was allotted to our team for developing this system, we did not have an opportunity to optimize several aspects of the system so that the power produced would be maximized. However, in our research and analysis of the system, we have developed ideas for subjects that may require further investigation in the future that could greatly increase the amount of power produced by the system. Namely, we will discuss possibilities related to optimizing the blades, the outer casing, and adding a flow diffuser.

For the current hydroflow generator design, one of the most logical system features to try to optimize would be the blades. Perhaps the greatest limitation on the efficiency and power obtained by the system is introduced by the blades that we have used. These blades were originally heavy duty diesel truck radiator fan blades. These blades are

clearly not optimized for our situation because 1) they were designed to operate with air, and 2) they were designed to drive fluid, not be driven by it. Therefore, we recommend further research on optimizing the blades for our purpose. If, based on the future research, appropriate blades could be obtained off the shelf, the blades may not cost much more then the ones we have used.

As briefly discussed in the Final Design section, the amount of decrease in the diameter of the outer casing would need to be investigated. If changes in the outer casing design could increase the flow rate and flow velocity, then the amount of power extracted by the blades could be increased as well. However, as described in the Final Design section, two different principles operate against each other as the exit diameter is decreased more and more. On the one hand, decreasing the exit diameter should increase the flow velocity because of continuity:

$$V_{EXIT} = \frac{V_{IN} A_{IN}}{A_{EXIT}} \quad \text{Eq. 17}$$

On the other hand, the decrease in the diameter would increase the pressure in the casing such that the pressure would push against the incoming flow and thereby decrease the flow into the casing. If either further testing or a computational fluid analysis is performed, an optimal amount of decrease in diameter could be determined so that the output power is maximized.

Another potential method of increasing the flow is by adding a diffuser behind the exit of the casing. The flow diffuser increases the area for the flow in such a way that the pressure would be decreased significantly. If a flow diffuser is added to the exit end of the hydroflow generator, the pressure after the hydroflow generator would be decreased so that the flow would be "pulled" out into the flow diffuser. This works just like how water is sucked through a straw by decreasing the pressure at the top of the straw. This pulling effect from the pressure drop would help increase the flow through the hydroflow generator and thereby increase the power extracted by the unit. Therefore, we recommend further investigation into incorporating a flow diffuser into this system. If this principle can successfully improve the unit, then the specific characteristics for the optimal flow diffuser would need to be determined by computational fluids analysis, testing, or more in-depth research on flow diffusers.

Conclusions

Since it is dangerous to continue supplying the power needs of remote Alaskan research camps by transporting gasoline, MHL wants to develop a portable hydroelectric generator to extract power from nearby rivers instead. MHL has requested our assistance in designing and fabricating this machine to produce around 10 kW of power while remaining lighter than 500 lbs.

After brainstorming to generate the different concepts for each separate component, we utilized a Pugh chart to help eliminate inferior concepts. In addition to this, we performed engineering analyses improve our understanding of the characteristics of our

final selected concept. From our analyses, we have determined that generating 10 kW of power with the given blades was not possible (See appendix E). Also, we determined that at flow velocity of around 4 m/s, the flow would exert nearly 2000 Newtons of force on the unit. Using this data we performed a cantilever beam bending stress analysis and determined that our connecting rods have a safety factor of 3.27 at the worst case scenario. Following these analyses, we tested the characteristics of our blades in MHL's testing basin. Based on the results from testing, we determined the most suitable gearing ratio (9:1) and commercially available generator for our unit. Upon procuring our parts, technicians at MHL helped us fabricate a first prototype, which we then tested to determine the power extraction capabilities of our system.

Based on results from our analysis and testing, we determined that our hydroflow generator should operate at efficiencies around the range of 15 % when both blades are used. This result prompted further research and scrutiny of our system. From this inspection of our system, we developed recommendations for future improvements, which include:

1) Research for optimizing turbine blades
2) Determination of optimal outer casing profile
3) Analysis for incorporating a diffuser into the system

Acknowledgments

We would like to thank Professor Guy Meadows for sponsoring our project. His willingness and flexibility to meet and discuss the project as well as granting us access to the facilities at the Michigan Hydrodynamic Laboratory contributed greatly to our efforts. We would also like to thank all the staff at the MHL for all their help with construction and testing of the prototype. The effort and time they put into this project was essential for its success. Moreover, we would like to thank Professor Katsuo Kurabayashi, who provided guidance on our fluids analysis along with advice for all aspects of our project.

References

[1] Platypus Power®, "240V AC Models", from http://www.platypuspower.com.au/m1.html, Retrieved on Jan. 20, 2007.

[2] B. R. Munson, D. F. Young, T.H. Okiishi, "Fundamentals of Fluid Mechanics." 5th ed. Danvers, MA, 2006.

Team Bios

Jacob Gore

Jacob Gore is a student in the School of Engineering at the University of Michigan in Ann Arbor Michigan. He majors in Mechanical Engineering and Industrial and Operations Engineering. Jacob was born in Nashville, Tennessee and has moved many times around the country with his family. His family currently resides in Saline, Michigan, right outside of Ann Arbor. He has an interest in the manufacturing and process flow of a wide range of consumer and industrial products. He has interned with Mitsubishi Motors R & D Laboratory in Ann Arbor, Michigan, doing research on audio and human interface systems of automobiles. He also has interned with Lutron GL in Shanghai, China, measuring performance of manufacturing process flow at the assembly lines there. His future career goals are to work for a large company in engineering consulting, whether it be supply chain analysis or leaning an existing manufacturing process.

Eric Lankheet

Eric Lankheet is a senior in mechanical engineering at the University of Michigan. He originally comes from Grand Blanc located south of Flint in Michigan. He first became interested in engineering through his father who is also a mechanical engineering graduate of the University of Michigan. His main interests are design and manufacturing and looks forward to working in this area in the future. He graduates in April 2007 and is looking to enter industry. Outside of the academic field his main interests are sports, more specifically football baseball and snowboarding, though he has not been able to participate in the latter much due to the mild winter.

Jason Riggs

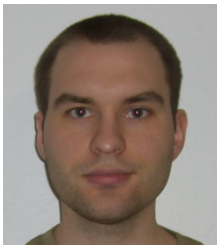

Born and raised in St. Louis, MO, Jason Riggs is currently a senior in mechanical engineering at the University of Michigan. His major interest lies in the area of mechanical design. He is the director of research for the Michigan Mars Rover Team, where most of his efforts have gone towards developing a modular rover design. He is also an avid guitarist/songwriter and volunteers regularly at The Ark, a small non-profit music venue in downtown Ann Arbor. After graduation, he hopes to obtain a position in the area of design of mechanical or electromechanical systems as well as to continue his education.

Ching-shih Yang

Ching-shih was born in Washington D.C. to a family which then moved to Taiwan, Texas, and then back to Taiwan again. After attending a bilingual school in Hsinchu, Taiwan, Ching-shih moved to Ann Arbor to begin studying Mechanical Engineering at the University of Michigan. In addition to his studies at U of M, Ching-shih actively participates in the Christians on Campus student organization. Expecting to graduate in April of 2007, Ching-shih has applied for the Sequential Graduate/Undergraduate program. If accepted to this program, Ching-shih expects to graduate in April of 2008 with a Master's degree in Mechanical Engineering. Ching-shih has been in a Co-op program with the Environmental Protection Agency since January of 2006. He hopes to work at the National Renewable Energy Laboratory sometime in the near future in order to do work related to the topic of his interest: renewable energy.

Appendix A: Concept Descriptions[1]

Energy Extraction:

- Waterwheel: Waterwheel with axis of rotation that's perpendicular to the river flow. River flow spins waterwheel, which could either directly run an electrical generator, a pump, or an air compressor, depending on the energy transfer component selected.

Energy Transfer:

- Electrical generator/ circuit: An electrical generator would be driven by the energy extraction component. The current would then be carried by the circuit to the energy storage component.

- Air compressor/ pneumatic circuit: An air compressor would be driven by the energy extraction component. The pneumatic circuit would carry the pressurized air to the energy storage component, which will be a compressed air storage tank.

- Water pump/ flowing water: The energy extraction component would drive the water pump, which would the pump water up to a higher elevation in a water tank.

Energy Storage:

- Hydraulic accumulator: A pressure vessel designed to store energy in the form of pressurized fluid.

- Battery array: An array of batteries. The Uninterruptible Power Supply, UPS, is a type of battery that could store and dispense power at the appropriate times, according to the research camp's needs.

- Compressed air storage tank: Energy stored in the form of compressed air. This concept is similar in theory to the hydraulic accumulator concept.

Energy Dissipation:

- Hydraulic generator: A commercially available hydraulic generator could produce the desired AC current output when we incorporate this unit into the hydraulic circuit.

- Air driven tools or compressed air generator: With a pneumatic circuit, if compressed air generators are commercially available, then pressurized air could be used to generate an electric current. When needed, this setup could potentially allow the use for air driven tools by directly connecting the tools to the pneumatic circuit.

- Heater/ water boiler: When the power extracted isn't being used, it could be dissipated in the form of heat to heat water or the living quarters. This energy dissipation concept could be used with any other energy dissipation method whenever there's power being produced that isn't being used.

- High-head/ low flow hydroelectric generator: These are commercially available. See Figure 2 for an example of such a unit.

[1] Except for concepts already described in Concept Generation section.

Appendix B: Test Data – Round 2

6:1 ratio pitch 50 degrees					
speed (ft/s)	Speed (m/s)	RPM	Voltage	Load (ohms)	Power (W)
3	0.9144	240	12.7	infinite	n/a
3	0.9144	160	3	0.8	11.25
5	1.524	450	23.2	infinite	n/a
5	1.524	350	7	0.8	61.25
7	2.1336	650	32.4	infinite	n/a
7	2.1336	515	10.8	0.8	145.8
8	2.4384	750	37	infinite	n/a
8	2.4384	640	12.7	0.8	201.6125
10	3.048	915	44.5	infinite	n/a
10	3.048	766	15.6	0.8	304.2
9:1 ratio 50 degree pitch					
Generator has 1.4 ohm internal resistance					
Speed (ft/s)	Speed (m/s)	RPM	Voltage (V)	Load (ohms)	Power (W)
3	0.9144	250	19.4	infinite	n/a
3	0.9144	150	3	0.8	11.25
5	1.524	400	35	infinite	n/a
5	1.524	400	7	0.8	61.25
7	2.1336	650	48	infinite	n/a
7	2.1336	460	12	0.8	180
8	2.4384	745	54.5	infinite	n/a
8	2.4384	550	14.4	0.8	259.2
10	3.048	900	66	infinite	n/a
10	3.048	700	18.5	0.8	427.8125
13	3.9624	1120	81.5	infinite	n/a
new resistance	6.4				
Speed (ft/s)	Speed (m/s)	RPM	Voltage (V)	Load (ohms)	Power (W)
7	2.1336	851	35.5	6.4	196.9140625
8	2.4384	972	41	6.4	262.65625
10	3.048	1236	51.2	6.4	409.6
11	3.3528	1341	55.5	6.4	481.2890625
new resistance	4.8				
Speed (ft/s)	Speed (m/s)	RPM	Voltage (V)	Load (ohms)	Power (W)
7	2.1336	809	32.5	4.8	220.0520833
8	2.4384	470	37.8	4.8	297.675
10	3.048	474	46.5	4.8	450.46875
11	3.3528	1315	50.8	4.8	537.6333333
13	3.9624	1522	57.8	4.8	n/a

Appendix C: Pugh Charts

		Energy Extraction			Energy Transfer			
		Turbine blades in parallel	Hydroflow generator	Water wheel	Hydraulic circuit	Air (pneumatic circuit)	Water	Electrical circuit
Customer Requirement	**Weight**							
Portable	9	0	0	-1	0	-1	-1	0
Durable	7	-1	0	1	0	0	0	0
Consistent power output	8	0	0	0	0	-1	-1	0
Ability to store excess output	8	0	0	0	0	-1	0	0
Small environmental impact	8	0	0	0	0	0	1	0
Easy setup	5	0	0	-1	0	-1	-1	1
Multi use	4	0	0	0	0	0	-1	0
Safe	10	0	0	0	0	0	1	-1
Robust	9	1	0	0	0	-1	-1	0
Low Cost	6	0	0	-1	0	1	-1	1
Sum		0	0	-2	0	-4	-4	1
Weighted Sum		2	0	-13	0	-33	-23	1

		Energy Storage				Energy Dissipation			
		Batteries	Hydraulic Accumulator	Compressed Air	Elevated water tank	Hydraulic generator	Air generator	Heated Water	Hydroelectric generator
Customer Requirement	**Weight**								
Portable	9	0	0	-1	-1	0	0	0	-1
Durable	7	1	0	0	-1	0	-1	0	0
Consistent power output	8	1	0	-1	-1	0	-1	0	-1
Ability to store excess output	8	1	0	-1	1	0	0	0	0
Small environmental impact	8	-1	0	1	1	0	1	1	1
Easy setup	5	0	0	-1	-1	0	0	-1	-1
Multi use	4	-1	0	1	-1	0	0	1	0
Safe	10	1	0	0	1	0	0	1	0
Robust	9	0	0	-1	-1	0	0	0	-1
Low Cost	6	-1	0	-1	-1	0	-1	-1	-1
Sum		1	0	-4	-4	0	-2	1	-4
Weighted Sum		15	0	-33	-22	0	-13	11	-29

Appendix D: Blade Testing Results and Blade Characteristics

Blade 1 (larger diameter, higher pitch angle)						Blade 2 (smaller diameter, lower pitch angle)					
Run	Speed (m/s)	Load (PSI)	Shaft RPM	Torque (NM)	Power (W)	Run	Speed (m/s)	Load (PSI)	Shaft RPM	Torque (NM)	Power (W)
1	0.610	0	5	0.366	0.192	1	0.608	10	0	11.509	0.000
2	1.254	0	120	-0.017	-0.210	2	1.212	10	65	24.019	163.490
3	1.882	0	179	-0.175	-3.282	3	1.815	10	161	26.096	439.980
4	2.507	0	235	-0.319	-7.849	4	2.419	10	235	24.739	608.797
5	0.630	10	0	14.556	0.000	5	1.211	20	0	45.583	0.000
6	1.256	10	85	22.433	199.679	6	1.209	12	54	28.060	158.673
7	1.884	9.5	157	24.128	396.696	7	1.818	12	150	33.006	518.459
8	2.508	10	220	21.311	490.970	8	2.420	12	224	33.814	793.190
9	1.264	20	11	51.955	59.848	9	1.213	14	34	33.166	118.088
10	1.258	12	70	29.920	219.326	10	1.882	14	139	40.597	590.929
11	1.882	12	149	32.443	506.224	11	2.421	14	220	40.639	936.255
12	2.508	12	213	30.680	684.337	12	1.212	18	0	43.479	0.000
13	2.508	12	215	29.687	668.398	13	1.819	18	110	55.287	636.856
14	1.259	14	42	36.594	160.950	14	3.027	10	299	24.932	780.636
15	1.882	14	140	41.125	602.928	15	1.517	12	105	32.185	353.891
16	2.508	14	202	42.824	905.864	16	2.119	12	191	33.076	661.561
17	1.256	18	22	44.448	102.400	17	2.724	12	263	33.210	914.652
18	1.884	18	118	57.705	713.054	18	2.117	14	179	41.343	774.976
19	1.258	22	0	56.701	0.000	19	2.724	14	254	43.175	1148.394

Blade number	Hub Diameter	Total Diameter	Pitch Angle
1	10.5 in.	26 in.	40˚
2	10.5 in.	24 in.	38˚

Appendix E: Theoretical Power Calculations

Speed(m/s)	Total Flow rate (kg/s)	Theoretical Total Power in Flow (W)	Actual Power From Testing	Efficiency
1.21	414.09	302.59	160.22	0.53
1.21	415.00	304.59	165.73	0.54
1.21	415.47	305.62	118.70	0.39
1.52	519.63	597.91	359.73	0.60
1.82	621.77	1024.37	453.70	0.44
1.82	622.69	1028.90	530.37	0.52
1.82	623.15	1031.21	643.26	0.62
1.88	644.48	1140.74	601.16	0.53
2.12	725.11	1624.68	791.94	0.49
2.12	725.69	1628.57	680.87	0.42
2.42	828.71	2425.31	638.03	0.26
2.42	829.03	2428.17	819.75	0.34
2.42	829.12	2428.94	961.88	0.40
2.72	932.96	3460.58	951.27	0.27
2.72	933.17	3462.88	1182.55	0.34
3.03	1036.79	4749.33	N/A	N/A
2	685.07	1370.14	N/A	N/A

Appendix F: Theoretical Power Calculations

V1	Total Flow rate (kg/s)	Theta1 (degrees)	Theta1(rad)	U1	W1	Vx1	Vtheta1	V2	Alpha	theta 2	theta 2(rad)	U2	W2	Vx2	Vtheta2	wshaft	Power(W)
0.5	171.3	40	0.70	0.42	0.65	0.5	0	0.5	1.43	85	1.48	0.42	0.82	0.07	0.49	0.21	17.78
1	342.5	40	0.70	0.84	1.31	1	0	1	1.43	85	1.48	0.84	1.64	0.14	0.99	0.83	142.23
1.5	513.8	40	0.70	1.26	1.96	1.5	0	1.5	1.43	85	1.48	1.26	2.47	0.21	1.48	1.87	480.02
2	685.1	40	0.70	1.68	2.61	2	0	2	1.43	85	1.48	1.68	3.29	0.29	1.98	3.32	1137.82
2.5	856.3	40	0.70	2.10	3.26	2.5	0	2.5	1.43	85	1.48	2.10	4.11	0.36	2.47	5.19	2222.30
3	1027.6	40	0.70	2.52	3.92	3	0	3	1.43	85	1.48	2.52	4.93	0.43	2.97	7.47	3840.13
3.5	1198.9	40	0.70	2.94	4.57	3.5	0	3.5	1.43	85	1.48	2.94	5.75	0.50	3.46	10.17	6097.98
4	1370.1	40	0.70	3.36	5.22	4	0	4	1.43	85	1.48	3.36	6.58	0.57	3.96	13.29	9102.53
0.5	171.3	45	0.79	0.5	0.71	0.5	0	0.5	1.42	85	1.48	0.5	0.85	0.07	0.49	0.25	21.17
1	342.5	45	0.79	1	1.41	1	0	1	1.42	85	1.48	1	1.70	0.15	0.99	0.99	169.37
1.5	513.8	45	0.79	1.5	2.12	1.5	0	1.5	1.42	85	1.48	1.5	2.55	0.22	1.48	2.23	571.62
2	685.1	45	0.79	2	2.83	2	0	2	1.42	85	1.48	2	3.41	0.30	1.98	3.96	1354.96
2.5	856.3	45	0.79	2.5	3.54	2.5	0	2.5	1.42	85	1.48	2.5	4.26	0.37	2.47	6.18	2646.40
3	1027.6	45	0.79	3	4.24	3	0	3	1.42	85	1.48	3	5.11	0.45	2.97	8.90	4572.98
3.5	1198.9	45	0.79	3.5	4.95	3.5	0	3.5	1.42	85	1.48	3.5	5.96	0.52	3.46	12.11	7261.72
4	1370.1	45	0.79	4	5.66	4	0	4	1.42	85	1.48	4	6.81	0.59	3.96	15.82	10839.65
0.5	171.3	50	0.87	0.60	0.78	0.5	0	0.5	1.42	85	1.48	0.60	0.88	0.08	0.49	0.29	25.21
1	342.5	50	0.87	1.19	1.56	1	0	1	1.42	85	1.48	1.19	1.77	0.15	0.99	1.18	201.67
1.5	513.8	50	0.87	1.79	2.33	1.5	0	1.5	1.42	85	1.48	1.79	2.65	0.23	1.48	2.65	680.63
2	685.1	50	0.87	2.38	3.11	2	0	2	1.42	85	1.48	2.38	3.54	0.31	1.98	4.71	1613.34
2.5	856.3	50	0.87	2.98	3.89	2.5	0	2.5	1.42	85	1.48	2.98	4.42	0.39	2.47	7.36	3151.06
3	1027.6	50	0.87	3.58	4.67	3	0	3	1.42	85	1.48	3.58	5.31	0.46	2.96	10.60	5445.03
3.5	1198.9	50	0.87	4.17	5.45	3.5	0	3.5	1.42	85	1.48	4.17	6.19	0.54	3.46	14.42	8646.50
4	1370.1	50	0.87	4.77	6.22	4	0	4	1.42	85	1.48	4.77	7.08	0.62	3.95	18.84	12906.73

Appendix G: Hydroflow Generator CAD Drawings

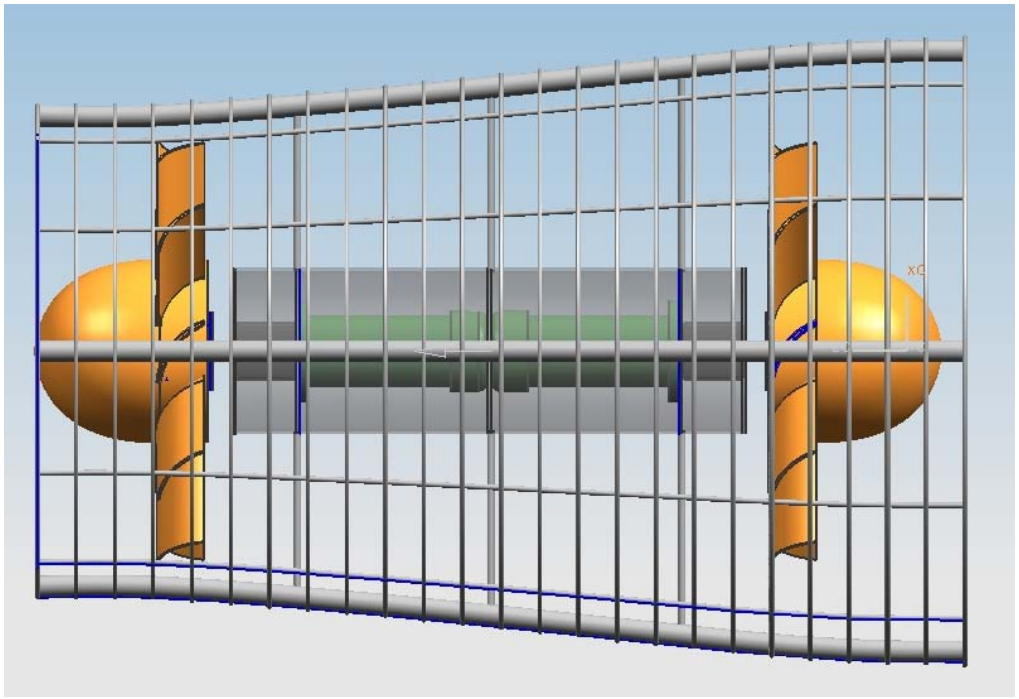

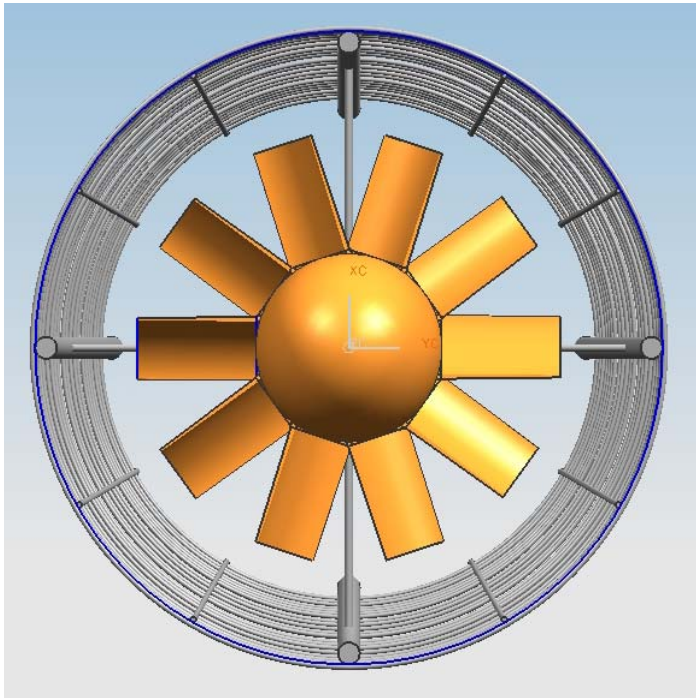

Appendix H: Hydroflow Generator Dimensioned CAD Drawings (Left View)

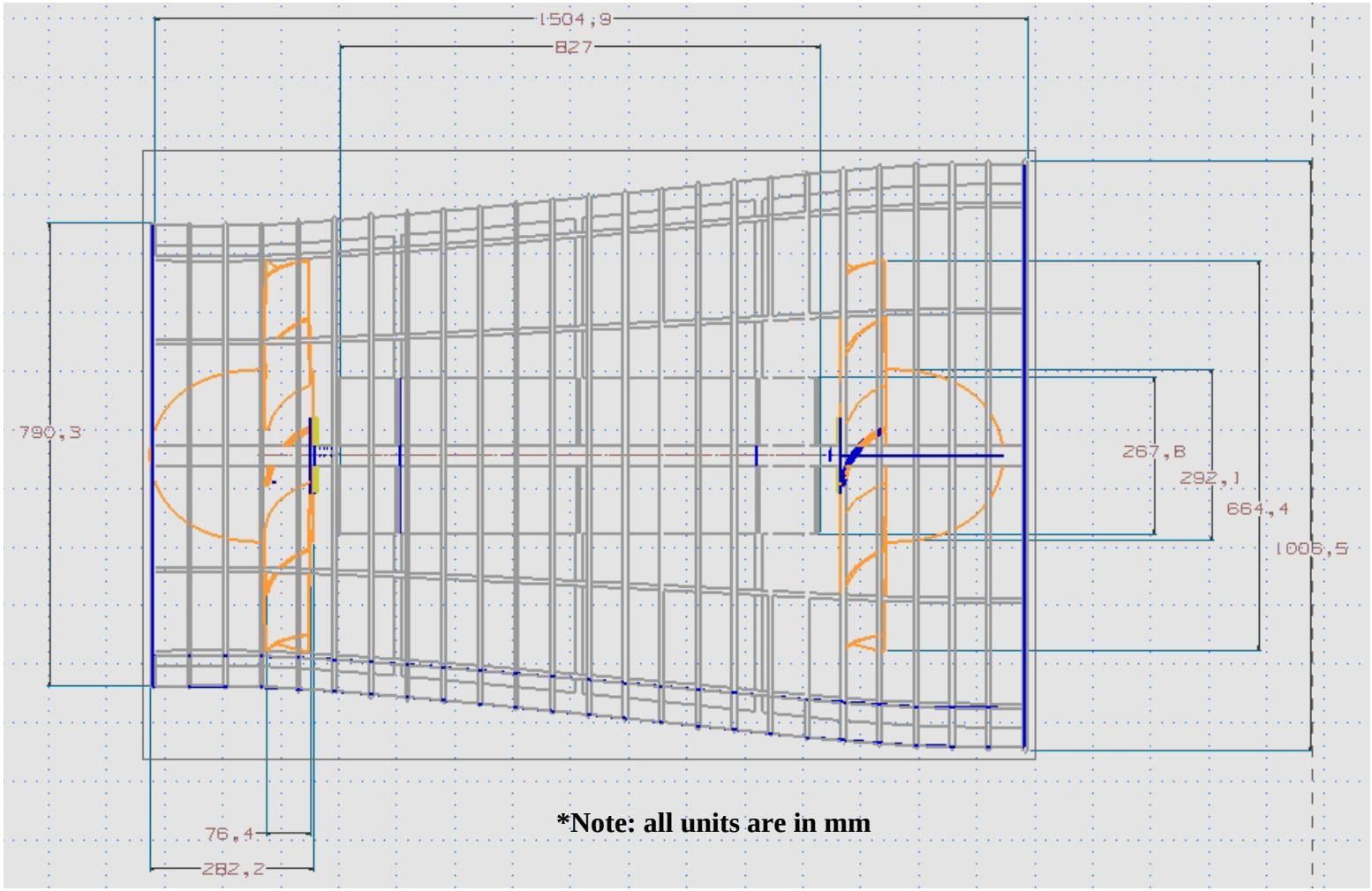

***Note: all units are in mm**

Appendix I: Hydroflow Generator Dimensioned CAD Drawings (Front View)

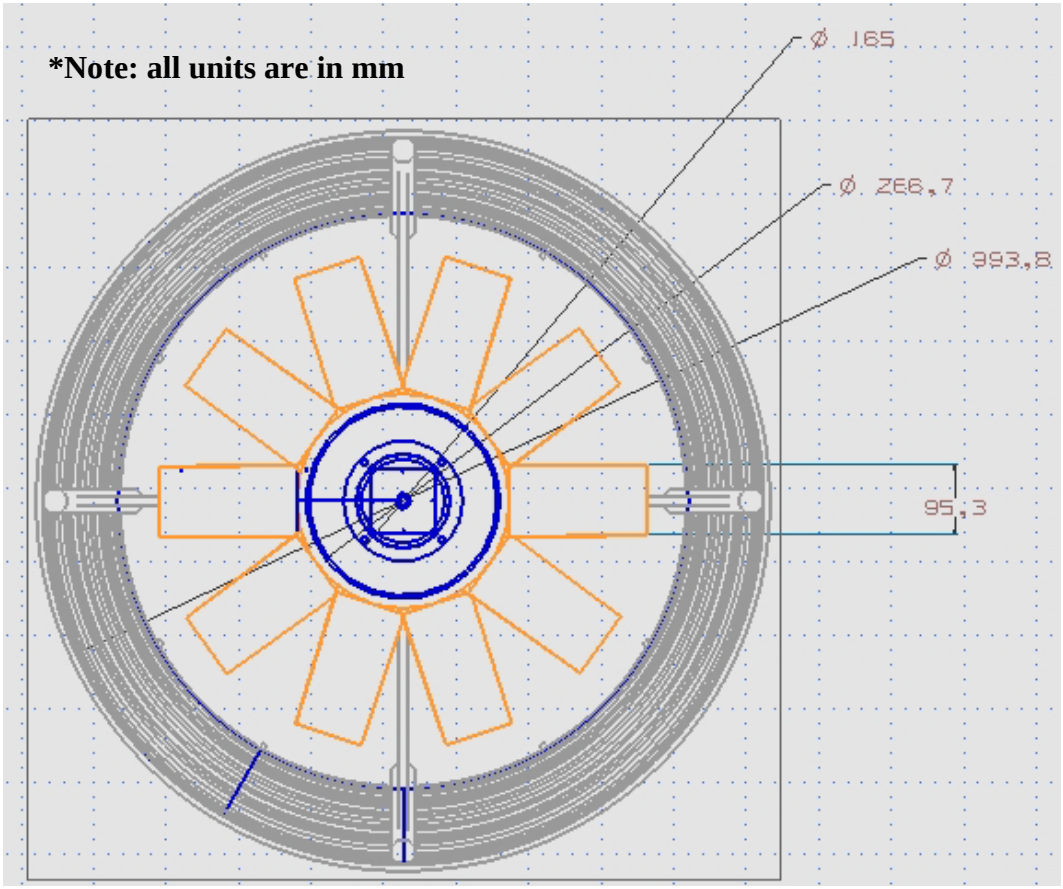

Appendix J: DC Generator Performance Characteristics